

The potential of vitamin K₃ as an anticancer agent against breast cancer that acts via the mitochondria-related apoptotic pathway

Takeshi Akiyoshi · Sumio Matzno · Mika Sakai ·
Noboru Okamura · Kenji Matsuyama

Received: 20 October 2008 / Accepted: 25 April 2009 / Published online: 16 May 2009
© Springer-Verlag 2009

Abstract

Purpose We tried to clarify the cytotoxic mechanism of VK₃ using the breast cancer cell line MCF-7.

Methods Cytotoxicity was measured via intracellular esterase activity. DNA fragmentation was assessed by agarose gel electrophoresis. JC-1 staining was applied to measure mitochondrial dysfunction. Caspase activation and reactive oxidative species (ROS) generation were also measured.

Results VK₃ exhibited cytotoxicity that caused DNA fragmentation in MCF-7 cells with an IC₅₀ of 14.2 μM. JC-1 staining revealed that VK₃ caused mitochondrial dysfunction including a disappearance of mitochondrial membrane potential. Additional investigation showed that the mitochondrial damage was induced by the generation of ROS and the subsequent activation of caspase-7 and -9.

Conclusions Our findings demonstrate that VK₃-induced apoptosis is selectively initiated by the mitochondria-related pathway and might be useful in breast cancer chemotherapy.

Keywords Vitamin K₃ · Breast cancer · ROS · Mitochondrial dysfunction

T. Akiyoshi · K. Matsuyama
Department of Clinical Pharmacy,
School of Pharmaceutical Sciences, Keio University,
1-5-30, Shibakoen, Minato-ku, Tokyo 105-8512, Japan

S. Matzno (✉) · M. Sakai · N. Okamura
School of Pharmaceutical Sciences,
Mukogawa Women's University, 11-68, Kyuban-cho,
Koshien, Nishinomiya, Hyogo 663-8179, Japan
e-mail: smatzno@mukogawa-u.ac.jp

S. Matzno · N. Okamura
The Joint Center of Industry and Mukogawa Women's University
for Developing Receptor Targeting Anticancer Agents, 11-68,
Kyuban-cho, Koshien, Nishinomiya, Hyogo 663-8179, Japan

Abbreviations

VK ₃	Vitamin K ₃
ROS	Reactive oxidative species
ER	Endoplasmic reticulum
HMEpC	Human mammary epithelial cells
DCFH-DA	2',7'-Dichlorofluorescein diacetate
FMK	Fluoromethylketone
AMC	7-Amino-4-methylcoumarin
DMSO	Dimethyl sulfoxide

Introduction

Vitamin K, an essential nutrient, has an important role in normal blood coagulation systems [1]. It acts as a cofactor of a number of plasma proteins such as prothrombin and factors VII, IX, and X. In recent years, several investigations have shown that vitamin K also possesses anticancer activity [2, 3]. Hemostatic proteins, such as thrombin, fibrin, and tissue factors play dual roles in both thrombosis formation and cancer progression [4, 5]. Chemically synthesized vitamin K₃ (2-methyl-1,4-naphthoquinone; VK₃) has a potent anticancer effect against various types of carcinoma, including hepatic, oral cavity, pharyngeal, mammary, breast, bladder, and blood cancers in vitro [3].

The cellular metabolism of VK₃ results in the formation of reactive oxygen species (ROS) including H₂O₂, O₂⁻, and OH, the highly deleterious hydroxyl radical, is generated in the presence of metal ions. The generated ROS cause various alterations including the induction of macromolecular damage, disruption of calcium homeostasis, depletion of cellular thiol levels, increases in lipid peroxidation, breaks in DNA, and cell death [6–10]. Regarding apoptosis, two pathways have been proposed; one is a mitochondrial-based pathway [11] and the other operates via the

endoplasmic reticulum (ER) [12] in normal pancreatic acinar cells.

Our goal in this study is to clarify the cytotoxic mechanism of VK_3 -induced cell death in breast cancer cells. Using the MCF-7 breast cancer cell line, we observed that VK_3 induces apoptosis involving DNA fragmentation in MCF-7 cells. This apoptosis was initiated via ROS production, and then followed by mitochondrial dysfunction and activation of the caspase-9-related apoptosis pathway. We also demonstrated that the intensity of apoptosis induced by VK_3 is twice as high in the breast cancer cell line MCF-7, than in normal mammary gland HMEpC epithelial cells.

Materials and methods

Cells and reagents

MCF-7 human breast cancer cells (passage up to 20) were provided by the Cell Resource Center for Biomedical Research, at the Institute of Development, Aging, and Cancer of Tohoku University. They were routinely maintained in a monolayer on plastic culture flasks at 37°C using minimum essential medium supplemented with 10% fetal calf serum, 100 IU/ml penicillin, and 100 µg/ml streptomycin. HMEpC human mammary epithelial cells (passage up to 15) were purchased from Toyobo Co. Ltd. (Osaka, Japan) and cultivated in the same manner as the MCF-7 cells.

Cell Counting Kit-F was obtained from Dojindo Laboratories (Kumamoto, Japan). VK_3 was purchased from Nacalai Tesque Inc. (Kyoto, Japan). Ac-LEVD-CHO, an inhibitor of caspase-4, was bought from Calbiochem (Darmstadt, Germany), z-DEVD-fluoromethylketone (FMK), an inhibitor of caspase-7, was obtained from Alexis Biochemicals (San Diego, CA), z-LEHD-FMK, an inhibitor of caspase-9 was purchased from R&D systems (Minneapolis, MN). Calpain-specific substrate Suc-LLVY-aminomethylcoumarin (AMC) was purchased from Bachem AG (Bubendorf, Germany). They were dissolved in dimethyl sulfoxide (DMSO) just before use. The final concentration of DMSO in the medium did not exceed 0.1% and did not affect cell viability (data not shown).

Anti-caspase-7 and 9 antibodies were obtained from Stress-Gen Biotechnologies (Ann Arbor, MI), and anti-caspase-4 antibody was acquired from Calbiochem. Peroxidase-conjugated anti-mouse and anti-rabbit IgG were purchased from Amersham Pharmacia Biotech (Arlington Heights, IL).

Cell viability assay

Cell Counting Kit-F was used to assess cell viability [13]. Briefly, cells were seeded onto 96 well microplates at a density of 1×10^4 cells/well and incubated for 24 h. The

cells were treated with VK_3 for a further 24 h. They were then washed with PBS and allowed to react with calcein-AM for 30 min. The released fluorescent calcein was measured in a CytoFluor® Plate Reader (PerSeptive Biosystems, Foster City, CA) using an excitation wavelength of 490 nm/emission 515 nm.

DNA fragmentation

The cells were plated onto 100 mm tissue culture dishes and treated with VK_3 for 24 h. They were then harvested with 100 µl lysis buffer (10 mM Tris-HCl, 10 mM EDTA, and 0.5% Triton X-100, adjusted to pH 7.4) for 20 min at 4°C. After centrifugation (15,000g for 5 min at 4°C), the supernatant was treated with 20 µg RNase A for 60 min at 37°C and subsequently with 20 µg proteinase K for 60 min at 50°C. After phenol-chloroform extraction, the fragmented DNA was precipitated with 0.4 M NaCl/50% isopropanol at -20°C and then electrophoresed on a 2% agarose gel containing 0.1 µg ethidium bromide and visualized under a 312 nm UV transilluminator.

Measurement of the population of apoptosis cells using sub- G_1 analysis

The sub- G_1 population was measured to quantify the number of apoptotic cells. After 24-h cultivation, adhered cells were trypsinized, washed with PBS, and fixed with 70% ethanol for 1 h at -20°C. After being washed with phosphate-citrate buffer (0.2 M Na_2HPO_4 and 0.1 M citric acid), the cells were treated with staining solution (PBS containing 3 µg/ml propidium iodide and 10 µg/ml RNase A) for 5 min at room temperature. The DNA content was then analyzed by flow cytometry (FACSCalibur™, Becton, Dickinson and Company, Franklin Lakes, NJ).

Measurement of caspase and calpain activity

Caspase activation was evaluated by the cleavage of pro-caspase proteins. To do so, immunoblot analysis was performed for the detection of cleaved caspase fragments as described previously [14]. Additional competitive experiments with caspase inhibitors were also applied to confirm the involvement of the three caspases during apoptosis. Briefly, cells were plated on a 96-well plate and cultured for 24 h. After treatment with caspase inhibitors for 30 min, they were incubated with VK_3 for more 6 h. The cell viability was assessed using Cell Counting Kit-F.

Calpain activity was determined using its specific substrate (Suc-LLVY-AMC) as described previously [14]. The enzyme activity of μ - and m-calpain was measured in the presence of 100 µM and 1 mM calcium, respectively.

Measurement of ROS

Reactive oxidative species generation was quantified with 2',7'-dichlorofluorescein diacetate (DCFH-DA) as a substrate for measuring intracellular oxidant production [15]. Briefly, MCF-7 cells were incubated with 15 μM VK₃ at 37°C in suspension culture for various time periods. After removing the VK₃, the cells were incubated with 20 μM DCFH-DA for 20 min. After removing the DCFH-DA and washing the cells with ice-cold PBS, the fluorescence was measured by excitation at 480 nm/emission 530 nm.

Intracellular ATP level

The intracellular ATP level was quantified by luciferase reagents using a luciferin/luciferase assay kit (Cellno, TOYOINK™, Tokyo, Japan) according to the manufacturer's instructions. Briefly, a 100 μl of luciferin/luciferase reagent solution was poured into the sample tubes, and the luminescent signal was measured with an MTP-700 Lab luminometer (CORONA Scientific Co. Ltd., Japan).

Measurement of mitochondrial membrane potential

J-aggregate-forming lipophilic cation (JC-1) was used to evaluate mitochondrial damage [16]. The uptake of JC-1 into mitochondria and the subsequent formation of J-aggregates is caused by high mitochondrial potential, and thus, this cationic dye is used to evaluate mitochondrial dysfunction.

Cells were seeded onto cover slips and treated with 15 μM VK₃ for 20, 40, 60, or 120 min. They were incubated with 5 $\mu\text{g/ml}$ JC-1 at 37°C for a further 30 min. After washing the cells thrice with PBS, they were applied to fluorescence microscopic observation. The shifting of mitochondrial membrane potential was also quantified using flow cytometry (FACSCalibur™ flow cytometry system, Becton, Dickinson and Co., Franklin Lakes, NJ). Briefly, after incubation with VK₃, the cells were incubated with JC-1 for 15 min. After washing them twice with PBS, the adherent cells were trypsinized, and the suspension was subjected to flow cytometry. J-aggregates are detected as orange fluorescence, whereas J-monomers are detected as green fluorescence.

Statistical analysis

The data are expressed as the mean \pm SD. Statistical significance was compared with Dunnett's or Williams' multiple comparison method using an one-way or two-way analytical model. *P* values of <0.05 were considered to be statistically significant.

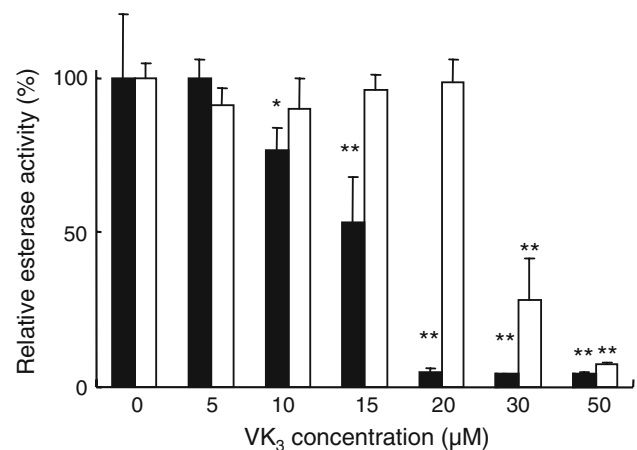


Fig. 1 Concentration-dependent cytotoxicity of VK₃ in MCF-7 (filled square) and HMEpC (open square) cells. The cells were treated with 0–50 μM VK₃ for 24 h, and then cell viability was assessed via cytosolic esterase activity. Values are expressed as the mean \pm SD (*n* = 5). Statistical significance from the control: **P* < 0.05, ***P* < 0.01

Results

Cytotoxicity of VK₃ in normal and tumor breast epithelial cells

Figure 1 shows the effects of VK₃ on the cell viability of MCF-7 and HMEpC cells using cytosolic esterase activity as an indicator. VK₃ reduced the enzyme activity of both the cells in a concentration-dependent manner. The IC₅₀ value was 14.2 μM for MCF-7 and 27.9 μM for HMEpC cells. Since VK₃ affects MCF-7 cells twice as much as HMEpC cells, this suggests the potential usefulness of VK₃ chemotherapy against breast cancer.

VK₃-induced apoptosis of MCF-7

Then, we evaluated the action mechanism of VK₃-induced cell death in MCF-7. Agarose gel electrophoresis revealed that VK₃ caused concentration-dependent apoptosis involving DNA fragmentation (Fig. 2a), especially at 20 μM VK₃ exposure for 24 h. The DNA fragmentation was also quantified using flow cytometry analysis. As shown in Fig. 2b, the sub-G₁ population was increased by the treatment of VK₃ for 24 h at concentrations of 1–20 μM . These results indicate that VK₃ induces apoptosis, although necrosis might occur at the higher concentration of 30 μM in MCF-7 cells.

In addition, we investigated caspase dependency during this apoptosis. Immunoblot analysis was applied to detect caspase cleavage. Fifteen micromoles of VK₃-induced

Fig. 2 Vitamin K₃-induced apoptotic DNA fragmentation in MCF-7 cells. **a** Cells were treated with 10–30 μ M drugs for 24 h, and then the nuclear DNA was electrophoresed onto 2% agarose gel. *M* 100-bp DNA ladder marker. **b** Quantitative evaluation of apoptosis in VK₃-treated MCF-7 cells. The cells were cultured in GM with 0–20 μ M VK₃ for 24 h followed by fixation with 70% ethanol. The sub-G₁ population was then analyzed using flow cytometry. Values represent mean \pm SD ($n = 8$) ** $P < 0.01$ versus control, as assessed by Williams' multiple comparison test

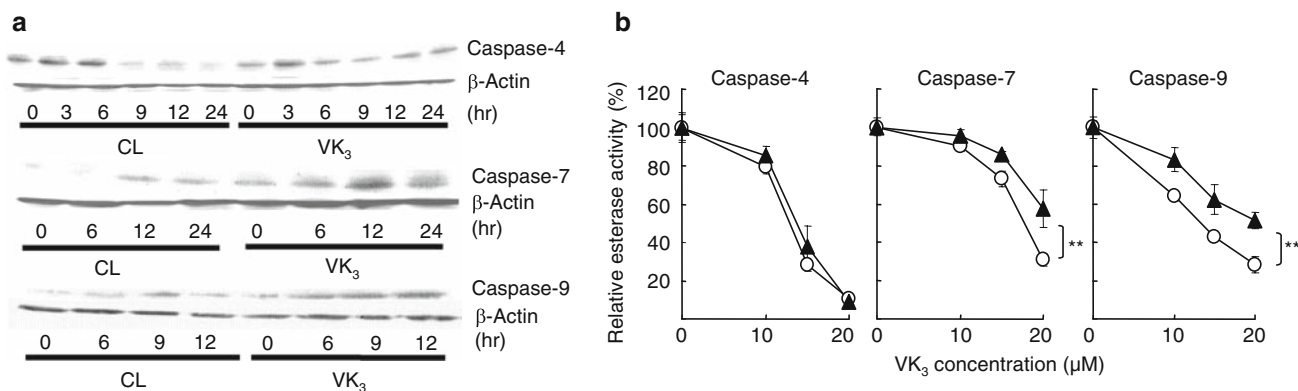
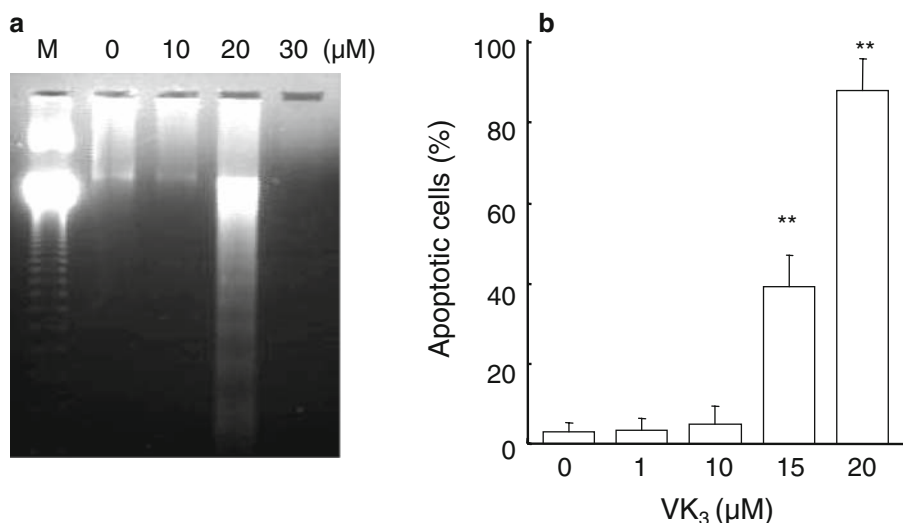


Fig. 3 Examination for the participation of various caspase cascades during VK₃-induced MCF-7 apoptosis. **a** Caspase cleavage was visualized using Western blotting analysis. Cells were treated with 15 μ M VK₃. Cleaved caspase-4 (top), 7 (middle), and 9 (bottom) were detected with their specific antibodies. **b** The protecting effect of caspase-specific inhibitors on VK₃-induced cytotoxicity. The cells were

incubated with (filled triangle) or without (open circle) 50 μ M caspase-4, 7, and 9 inhibitors for 30 min followed by treatment with VK₃ for 6 h. Cell viability was then assessed using Calcein-AM. Values represent the mean \pm SD ($n = 6$). Statistical significance was assessed by two-way ANOVA; ** $P < 0.01$

cleavage of caspase-7 and 9 from 6 h onwards in MCF-7 cells, whereas caspase-4 cleavage was not observed during the 24-h treatment period (Fig. 3a). An additional cell viability assay was done using their specific caspase inhibitors (Fig. 3b). VK₃-induced cell death was significantly reduced with specific inhibitors of caspase-7 and 9, whereas the caspase-4 inhibitor did not have any effects. Further, we measured the cytosolic calpain activity, which is activated by cleaved caspase-4 in the ER stress-related caspase cascade [17]. Interestingly, both m-calpain and μ -calpain were time-dependently activated in MCF-7 cells; however, VK₃ did not affect their activity (Fig. 4). Taken together, our current observations suggest that mitochondrial damage followed by the induction of caspase-7 and 9, at least partly contributes to VK₃-induced apoptosis in MCF-7 cells.

The effects of VK₃ on intracellular ROS and ATP levels and mitochondrial membrane potentials in MCF-7 cells

As predicted above, VK₃ induces apoptosis in MCF-7 cells through mitochondrial failure. In order to confirm the hypothesis, we directly evaluated the effect of VK₃ on mitochondrial function. Mitochondrial dysfunction has been shown to lead to the generation of ROS, which could be a contributing factor to cell death [18, 19]. Therefore, we investigated whether ROS are generated in MCF-7 cells. When MCF-7 cells were treated with 15 μ M VK₃, a significant increase in intracellular ROS (Fig. 5a) and a decrease in ATP (Fig. 5b) occurred in a time-dependent manner. Therefore, we observed the mitochondrial membrane potential in the presence and absence of VK₃, using JC-1 cationic dye (Fig. 6). The control cells showed heterogeneous staining

Fig. 4 Effect of VK_3 on cytosolic calpain activity in MCF-7 cells. The cells were treated with (filled triangle) or without (open circle) $15 \mu M$ VK_3 for 0, 6, 9, 12, 15, or 18 h. They were then incubated with substrate buffer for 60 min and supplied for subsequent m- (a) and μ -calpain (b) analysis. Values represent the mean \pm SD ($n = 8$). Statistical significance was assessed by two-way ANOVA: * $P < 0.05$, ** $P < 0.01$

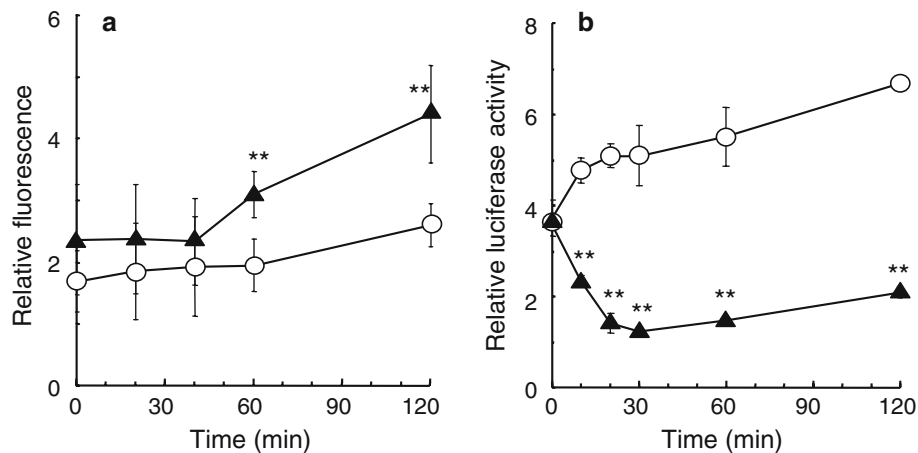
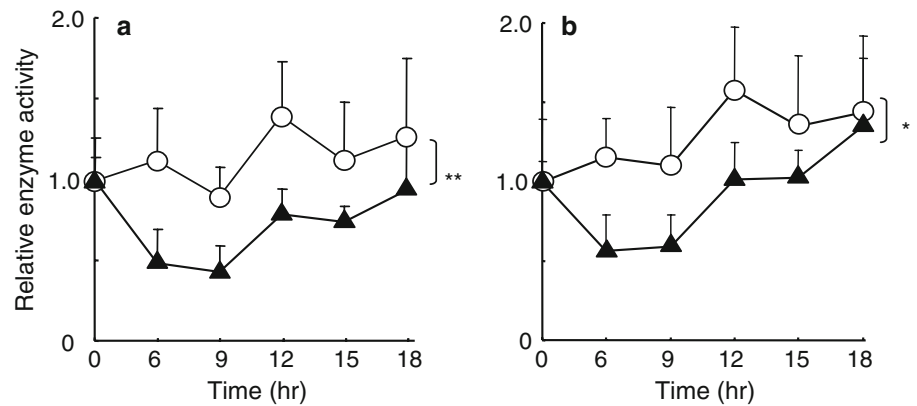


Fig. 5 Several intracellular changes associated with mitochondrial dysfunction. **a** VK_3 -induced ROS generation in MCF-7 cells. The cells were treated with (filled triangle) or without (open circle) $15 \mu M$ VK_3 for 20, 40, 60, or 120 min. Then, they were reacted with $20 \mu M$ DCFH-DA for 20 min. Values represent the mean \pm SD ($n = 4$) ** $P < 0.01$ versus control assessed by Williams' multiple comparison test.

b Rapid ATP decrease in VK_3 -treated MCF-7 cells. Cells were treated with (filled triangle) or without (open circle) $15 \mu M$ VK_3 . Intracellular ATP levels were measured using a luciferase-based bioluminescent assay. Values represent the mean \pm SD ($n = 4$) ** $P < 0.01$ versus control, as assessed by Dunnett's multiple comparison test

of the cytoplasm with both red and green fluorescence coexisting in the same cells (Fig. 6a–c). Exposure of the MCF-7 cells to $15 \mu M$ VK_3 for 6 h induced marked changes in mitochondrial potential as evident from the disappearance of red fluorescence and the increase in green fluorescence in most cells with a predominantly peripheral distribution. Several cells were devoid of red fluorescence, which is an indication of the loss of mitochondrial potential and the severity of cell damage caused by $15 \mu M$ VK_3 treatment for 6 h (Fig. 6d). These alterations induced mitochondrial dysfunction and a loss of mitochondrial membrane potential.

The mitochondrial damage was quantified by flow cytometry. JC-1-stained cells revealed a significantly increased green ratio in a time-dependent manner (Fig. 6e). These results indicate that VK_3 induces mitochondria dysfunction, probably through ROS, and resulting in apoptosis.

Discussion

In this study, the authors evaluated the potential of VK_3 as a chemotherapeutic agent against breast cancer cells. Indeed, in the MCF-7 human breast cancer cell line, VK_3 caused a dose-dependent cytotoxicity at an IC_{50} value of $14.2 \mu M$ (Fig. 1). This cytotoxicity was induced through nuclear DNA fragmentation (Fig. 2) suggesting that VK_3 causes cell death in MCF-7 by apoptosis. Our previous report indicated that VK_3 also possesses cytotoxic activity in the Hep G2 human hepatoblastoma cell line with a similar IC_{50} value [20]. On the other hand, VK_3 has a lower cytotoxicity against HMEpC cells with an IC_{50} of $27.9 \mu M$ (Fig. 1b), which is twice as high as that of MCF-7 cells. Therefore, these observations suggest that VK_3 has the potential to be used as a wide-spectrum chemotherapeutic agent against recalcitrant solid carcinoma. Salido et al. [21] suggested that ROS generated by VK_3 induce growth suppression that

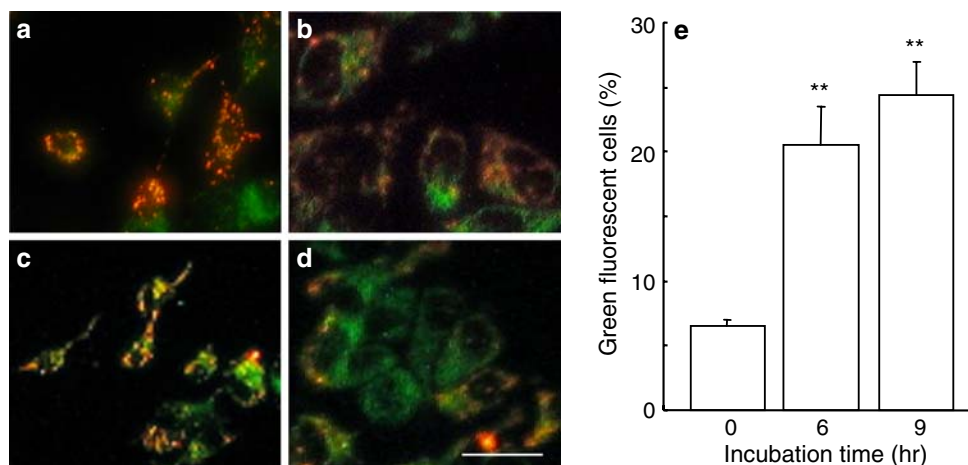


Fig. 6 VK₃ caused the loss of mitochondrial membrane potential. Fluorescence microscopic observation of JC-1-stained MCF-7 cells: control at 0 (a) and 6 h (c), 15 μM VK₃ treatment for 0 (b) and 6 h (d). Functional mitochondria containing J-aggregates were stained orange, whereas damaged mitochondria containing J-monomers were stained

green. var: 10 μm. **e** Quantitative analysis of JC-1-stained cells using flow cytometry. The cells were incubated with 15 μM VK₃ for 6 and 9 h and then, they were stained with JC-1 for 15 min. Values represent the mean ± SD (n = 5). **P < 0.01 versus control, as assessed by Williams' multiple comparison test

includes the direct suppression of mitochondrial function. In general, mitochondrial defects have long been suspected to play an important role in the development and progression of cancer. Indeed, due to the inherent inefficiency of glycolytic ATP generation, malignant cells require a high amount of glucose to fulfill their cellular energy requirements. Therefore, the differences in energy metabolism between normal and cancer cells constitute a biochemical basis to speculate that therapeutic strategies might be developed to selectively kill cancer cells via their inherently compromised respiratory state [22–25]. Taken together, VK₃ might induce severer cytotoxicity in carcinoma cells than in normal cells.

We next investigated the mechanism of action of VK₃-induced apoptosis in MCF-7 cells. Generally, three main caspase cascades induce irreversible apoptosis: the 'death ligand'-mediated pathway through caspase-8, the mitochondrial damage-induced pathway through caspase-9, and the ER stress-related pathway through caspase-12 [26]. The caspase molecules transmit apoptotic signals in a manner that transcends species differences [27]. In humans, caspase-4 mediates apoptosis specifically in response to ER stress in Alzheimer's disease [17, 28] and in neuronal ceroid lipofuscinoses, commonly known as Batten disease [29]. Caspase-7 is considered to be the downstream and ultimate apoptosis factor in the mitochondrial pathway in MCF-7 cells [30].

Based on the above information, we measured the activation of various caspases in MCF-7 cells (Fig. 3). VK₃ activated caspase-7 and 9, whereas it did not cleave the caspase-4 molecule. In addition, inhibition of these caspases recovered cell viability (Fig. 3b). These findings

indicate that the mitochondrial pathway plays a central role in VK₃-induced apoptosis. In order to check this hypothesis, we examined mitochondrial function in VK₃-treated MCF-7 cells. VK₃ generated intracellular ROS quickly and decreased the intracellular ATP level (Fig. 5). Finally, a fluorescent dye assay using JC-1 (Fig. 6) directly detected that VK₃ caused mitochondrial dysfunction accompanied by the disappearance of membrane potential, which is essential for mitochondrial energy production.

It is unclear whether VK₃ accumulates in breast cancer cells. Although VK₃ is quite lipophilic and conceivably distributes to various organ, the distribution to breast cancer may not exceed to other organs. However, previous reports showed that VK₃ is rapidly conjugated to intracellular glutathione via nucleophilic reaction to form a stable conjugate and the loss of viability of Hep G2 cells upon exposure to VK₃ is preceded by rapid depletion of intracellular glutathione [31, 32]. This glutathione decrement was caused by the conjugation of glutathione to VK₃ or the oxidation of glutathione to the disulfide form [33]. The S conjugate, thiiodione, is hydrophilic and thus does not permeate the plasma membrane by passive diffusion.

In addition, our personal data also showed that the intracellular ATP level was not decreased by the addition of VK₃ to HMEpC cells (data not shown). This suggests VK₃ preferentially affects breast adenocarcinoma rather than normal mammary gland. Because this report focused on the mechanism of cytotoxicity induced by VK₃ in cancer cells, we did not describe this observation in the current manuscript.

Park et al. [34] reported similar apoptosis results in VK₃-treated cardiomyoblast cells, i.e., VK₃-induced apoptosis

caused by mitochondrial dysfunction due to generated ROS. In general, mitochondria have two essential functions during apoptosis: (1) energy production in the form of ATP, which is required by all cells that die via an apoptotic pathway and (2) proapoptotic proteins are sequestered into the intermembrane space of the cytosol, in which they trigger downstream apoptotic signaling pathways [17, 35–39]. In addition, apoptosis is accompanied by signs of mitochondrial dysfunction, including a loss of the inner mitochondrial transmembrane potential; the release of soluble intermembrane proteins, including cytochrome c; and caspase-9 activation [40–42].

Several investigators have shown that ROS are also induced by ER stress-related calcium ion leakage [12] and the subsequent activation of calpains and caspase-4, which are signal factors related to apoptosis [17]. In contrast, Obeng and Boise [43] suggested that caspase-4 activation is not required for the induction of ER stress-induced apoptosis. VK₃-induced apoptosis in MCF-7 cells might be not necessary for the activation of the ER. Our results only revealed that VK₃ generated ROS, causing mitochondrial dysfunction (Figs. 5a, 6). Before this, caspase-9 activation followed by the caspase-7 activation occurred. In contrast, caspase-4 activation was not observed suggesting that VK₃-induced apoptosis is mainly triggered by mitochondrial damage and is independent of the ER stress-related pathway. Further investigation is needed to confirm the effects of VK₃ on mitochondrial function.

In conclusion, VK₃ caused apoptosis in breast tumor cells via the mitochondria-related pathway. Its potency is as twice high in MCF-7 cells than in normal breast epithelial cells, and thus, it might be useful for chemotherapy in breast cancer patients.

Acknowledgments This work was supported by a Grant-in-Aid for Scientific Research from the Ministry of Education, Culture, Sports, Science, and Technology of Japan.

References

1. Cranenburg EC, Schurgers LJ, Vermeer C (2007) Vitamin K: the coagulation vitamin that became omnipotent. *Thromb Haemost* 98:120–125
2. Falanga A (2003) Biological and clinical aspects of anticancer effects of antithrombotics. *Pathophysiol Haemost Thromb* 33:389–392
3. Lamson DW, Plaza SM (2003) The anticancer effects of vitamin K. *Altern Med Rev* 8:303–318
4. Falanga A, Marchetti M, Vignoli A et al (2003) Clotting mechanisms and cancer: implications in thrombus formation and tumor progression. *Clin Adv Hematol Oncol* 1:673–678
5. Piccioli A, Falanga A, Prandoni P (2006) Anticoagulants and cancer survival. *Semin Thromb Hemost* 32:810–813
6. Tzeng WF, Chiou TJ, Huang JY et al (1992) Menadione-induced cardiotoxicity is associated with alteration in intracellular Ca²⁺ homeostasis. *Proc Natl Sci Counc Repub China B* 16:84–90
7. Tzeng WF, Chiou TJ, Wang CP et al (1994) Cellular thiols as a determinant of responsiveness to menadione in cardiomyocytes. *J Mol Cell Cardiol* 26:889–897
8. Tzeng WF, Lee JL, Chiou TJ (1995) The role of lipid peroxidation in menadione-mediated toxicity in cardiomyocytes. *J Mol Cell Cardiol* 27:1999–2008
9. Chiou TJ, Tzeng WF (2000) The roles of glutathione and antioxidant enzymes in menadione-induced oxidative stress. *Toxicology* 154:75–84
10. D'Odorico A, Sturniolo GC, Bilton RF et al (1997) Quinone-induced DNA single strand breaks in a human colon carcinoma cell line. *Carcinogenesis* 18:43–46
11. Dussmann H, Kogel D, Rehm M et al (2003) Mitochondrial membrane permeabilization and superoxide production during apoptosis: a single-cell analysis. *J Biol Chem* 278:12645–12649
12. Gerasimenko JV, Gerasimenko OV, Palejwala A et al (2002) Menadione-induced apoptosis: roles of cytosolic Ca²⁺ elevations and the mitochondrial permeability transition pore. *J Cell Sci* 115:485–497
13. Sakamoto S, Yokoyama M, Zhang X et al (2004) Increased expression of CYR61, an extracellular matrix signaling protein, in human benign prostatic hyperplasia and its regulation by lysophosphatidic acid. *Endocrinology* 145:2929–2940
14. Matzno S, Yasuda S, Kitada Y et al (2006) Clofibrate-induced apoptosis is mediated by Ca²⁺-dependent caspase-12 activation. *Life Sci* 78:1892–1899
15. Robinson JP, Bruner LH, Bassoe CF et al (1988) Measurement of intracellular fluorescence of human monocytes relative to oxidative metabolism. *J Leukoc Biol* 43:304–310
16. Smiley ST, Reers M, Mottola-Hartshorn C et al (1991) Intracellular heterogeneity in mitochondrial membrane potentials revealed by a J-aggregate-forming lipophilic cation JC-1. *Proc Natl Acad Sci USA* 88:3671–3675
17. Hitomi J, Katayama T, Eguchi Y et al (2004) Involvement of caspase-4 in endoplasmic reticulum stress-induced apoptosis and Abeta-induced cell death. *J Cell Biol* 165:347–356
18. Green DR, Reed JC (1998) Mitochondria and apoptosis. *Science* 281:1309–1312
19. Zamzami N, Marchetti P, Castedo M et al (1995) Sequential reduction of mitochondrial transmembrane potential and generation of reactive oxygen species in early programmed cell death. *J Exp Med* 181:367–377
20. Matzno S, Yamaguchi Y, Akiyoshi T et al (2008) An attempt to evaluate the effect of vitamin K₃ using as an enhancer of anticancer agents. *Biol Pharm Bull* 31:1270–1273
21. Salido M, Gonzalez JL, Vilches J (2007) Loss of mitochondrial membrane potential is inhibited by bombesin in etoposide-induced apoptosis in PC-3 prostate carcinoma cells. *Mol Cancer Ther* 6:1292–1299
22. Warburg O (1930) *The metabolism of tumors*. London Constable Co. Ltd, London
23. Warburg O (1956) On the origin of cancer cells. *Science* 123:309–314
24. Hockenbery DM (2002) A mitochondrial achilles heel in cancer? *Cancer Cell* 2:1–2
25. Carew JS, Huang P (2002) Mitochondrial defects in cancer. *Mol Cancer* 1:9
26. Alberts B, Johnson A, Lewis J et al (2002) The cell cycle and programmed cell death. In: *Molecular biology of the cell*, 4th edn. Garland Science, New York, pp 983–1026
27. Alnemri ES, Livingston DJ, Nicholson DW et al (1996) Human ICE/CED-3 protease nomenclature. *Cell* 18:171
28. Katayama T, Imaizumi K, Manabe T et al (2004) Induction of neuronal death by ER stress in Alzheimer's disease. *J Chem Neuroanat* 28:67–78

29. Kim SJ, Zhang Z, Hitomi E et al (2006) Endoplasmic reticulum stress-induced caspase-4 activation mediates apoptosis and neurodegeneration in INCL. *Hum Mol Genet* 15:1826–1834
30. Liang Y, Yan C, Schor NF (2001) Apoptosis in the absence of caspase-3. *Oncogene* 4:6570–6578
31. Duthie SJ, Grant MH (1989) The toxicity of menadione and mitozantrone in human liver-derived Hep G2 hepatoma cells. *Biochem Pharmacol* 38:1247–1255
32. Mauzeroll J, Bard AJ, Owhadian O et al (2004) Menadione metabolism to thiodione in hepatoblastoma by scanning electrochemical microscopy. *Proc Natl Acad Sci USA* 101:17582–17587
33. Di Monte D, Ross D, Bellomo G et al (1984) Alterations in intracellular thiol homeostasis during the metabolism of menadione by isolated rat hepatocytes. *Arch Biochem Biophys* 235:334–342
34. Park C, So HS, Shin CH et al (2003) Quercetin protects the hydrogen peroxide-induced apoptosis via inhibition of mitochondrial dysfunction in H9c2 cardiomyoblast cells. *Biochem Pharmacol* 66:1287–1295
35. Petronilli V, Penzo D, Scorrano L et al (2001) The mitochondrial permeability transition, release of cytochrome *c* and cell death: correlation with the duration of pore openings in situ. *J Biol Chem* 276:12030–12034
36. James AM, Murphy MP (2002) How mitochondrial damage affects cell function. *J Biomed Sci* 9:475–487
37. Lim ML, Lum MG, Hansen TM et al (2002) On the release of cytochrome *c* from mitochondria during cell death signaling. *J Biomed Sci* 9:488–506
38. Lawen A (2003) Apoptosis an introduction. *Bioessays* 25:888–896
39. Kuznetsov AV, Usson Y, Leverage X et al (2004) Subcellular heterogeneity of mitochondrial function and dysfunction: evidence obtained by confocal imaging. *Mol Cell Biochem* 256–257:359–365
40. Green DR, Reed JC (1998) Mitochondria and apoptosis. *Science* 281:1309–1312
41. Kroemer G, Dallaporta B, Resche-Rigon M (1998) The mitochondrial death/life regulator in apoptosis and necrosis. *Annu Rev Physiol* 60:619–642
42. Gross A, McDonnell JM, Korsmeyer SJ (1999) BCL-2 family members and the mitochondria in apoptosis. *Genes Dev* 13:1899–1911
43. Obeng EA, Boise LH (2005) Caspase-12 and caspase-4 are not required for caspase-dependent endoplasmic reticulum stress-induced apoptosis. *J Biol Chem* 280:29578–29587